ARCHIVES OF ELECTRICAL ENGINEERING VOL. 68(1), pp. 63–75 (2019)

DOI 10.24425/aee.2019.125980

Stepper motor open-loop control system modeling and control strategy optimization

DAODE ZHANG, JINGQI WANG, LEI QIAN, JUN YI

School of Mechanical Engineering, Hubei University of Technology, China
e-mail: zhangdaode012@yeah.net

(Received: 27.07.2018, revised: 15.10.2018)

Abstract: The study of the subdivision driving technology of a stepper motor and two types of typical acceleration and deceleration curves aims at optimizing the open-loop control performance of the stepper motor. The simulation model of a two-phase hybrid stepper motor open-loop control system is set up based on the mathematical model of the stepper motor, in order to let the stepper motor have the smaller stepper angle, two types of typical acceleration and a deceleration curve algorithm are designed for the real-time online calculation based on the subdivision driving technology. It respectively carries out the simulation analysis for their control effects. The simulation results show that the parabolic acceleration and deceleration curves have a larger maximum in-step rotation angle and the faster dynamic response ability in the same control period, and at the same time, the position tracking error of an intermediate process is smaller.

Key words: acceleration and deceleration control, open loop control, stepper motor, subdivision control, system modeling

1. Introduction

A stepper motor is a kind of open-loop control motor which can translate the digital pulse signal to the corresponding displacement increment; it is a major actuating element and power element [1] in a modern digital control system.

The control method of a stepping motor includes open-loop control and closed-loop control. The closed-loop method forms the closed-loop through detecting the position of a motor rotor, carries a fuzzy proportional-integral-derivative (PID), space vector pulse width modulation (SVPWM) and other control technology in the traditional closed-loop control to make the system have better control performance and dynamic response, but the complexity and cost of the closed-loop control system are higher [2–3]. The closed-loop control is the right choice stepper motor, it is used in complex applications where use is more important than cost [4]. With the development of subdivision driving technology and increasing maturity, it can reduce the motor step angle and eliminate surging at low frequency, thereby decreasing a machine pulse equivalent to improve

the precision of servo control and precision machining [5], and then through loading the suitable acceleration and deceleration control curves. The open-loop control method can also effectively avoid the motor vibration, step out and other phenomena. Due to its simple implementation, the system control precision and stability can meet most of the application demands, the open-loop control has become the main control way of the stepping motor.

This paper focuses on researching the two-phase hybrid stepper motor rotation system, sets up its open-loop control system simulation model, expounds the application of subdivision driving technology [6–10] in the system as well as its optimized simulation effect. It studies the acceleration and deceleration curve algorithm [11–15] applied for the real-time online calculation, it designs two types of typical acceleration and deceleration curve algorithm, and, respectively, carries out the simulation for their control performance through the comparison to analyze a better speed control curve algorithm.

2. Two-phase hybrid stepper motor control system modeling

Due to the fact that a stepper motor has a lot of nonlinear components; it is required to carry out the corresponding simplification for the model to better realize the correct motor control system modeling. The voltage equation [3] of a two-phase hybrid stepper motor can be shown as:

$$\begin{cases} U_A = R_A i_A + (L_0 - L_1 \cos 2\theta)\dfrac{\mathrm{d}i_A}{\mathrm{d}t} - L_1 \sin 2\theta \dfrac{\mathrm{d}i_B}{\mathrm{d}t} \\ \qquad + 2L_1 (i_A \sin 2\theta - i_B \cos 2\theta) - k_e w_r \sin\theta \\ U_B = R_B i_B + (L_0 + L_1 \cos 2\theta)\dfrac{\mathrm{d}i_B}{\mathrm{d}t} - L_1 \sin 2\theta \dfrac{\mathrm{d}i_A}{\mathrm{d}t} \\ \qquad - 2L_1 (i_A \sin 2\theta + i_B \cos 2\theta) + k_e w_r \cos\theta \end{cases} . \tag{1}$$

Therein, U_A, U_B are the voltage of the two-phase winding; R_A, R_B are the resistance of the two-phase winding; i_A, i_B are the current of the two-phase stator winding; L_0 is the self-inductance average component of the motor stator winding; L_1 is the self-inductance fundamental component of the stator winding; θ is the rotor real-time position; k_e is the counter electromotive force coefficient of the stepper motor; w_r is the mechanical angular velocity of the motor rotor.

The torque equation of the two-phase hybrid stepper motor is:

$$T_e = J\frac{\mathrm{d}w_r}{\mathrm{d}t} + Bw_r + T_L \,. \tag{2}$$

Therein, T_e is the electromagnetic torque of the motor; J is the rotational inertia of the motor; B is the friction coefficient of the motor; T_L is the additional load torque of the motor, and the electromagnetic torque T_e is composed by the reaction torque T_s generated from the stator winding, plus the permanent magnet torque T_m set up by the rotor, namely:

$$T_e = T_s + T_m \,. \tag{3}$$

The reaction torque T_s in the power-on state:

$$T_s = N_r \left(\frac{1}{2} i_A^2 \frac{\partial L_{AA}}{\partial \theta} + \frac{1}{2} i_B^2 \frac{\partial L_{BB}}{\partial \theta} + i_A i_B \frac{\partial M_{AB}}{\partial \theta} \right) . \tag{4}$$

Therein, N_r is the quantity of the upper teeth of the motor rotor; L_{AA}, L_{BB} and M_{AB} are, respectively, the self-inductance and mutual inductance between the stator two-phase winding.

The permanent magnet torque T_m is:

$$T_m = N_r \left(I_m i_A \frac{\partial M_{Am}}{\partial \theta} + I_m i_B \frac{\partial M_{Bm}}{\partial \theta} \right). \tag{5}$$

Therein, I_m is the field current of the rotor; M_{Am} and M_{Bm} are, respectively, the mutual inductance of the two-phase winding and rotor.

By plugging (4), (5) into (3), we can obtain:

$$\begin{aligned} T_e = T_s + T_m = N_r & \left(\frac{1}{2} i_A^2 \frac{\partial L_{AA}}{\partial \theta} + \frac{1}{2} i_B^2 \frac{\partial L_{BB}}{\partial \theta} + i_A i_B \frac{\partial M_{AB}}{\partial \theta} \right) \\ + N_r & \left(I_m i_A \frac{\partial M_{Am}}{\partial \theta} + I_m i_B \frac{\partial M_{Bm}}{\partial \theta} \right) \end{aligned} \tag{6}$$

and

$$\begin{cases} L_{AA} = L_0 - L_1 \cos 2\theta \\ L_{BB} = L_0 + L_1 \cos 2\theta \\ M_{AB} = M_{BA} = -L_1 \sin 2\theta \\ M_{Am} = M_{sr} \sin \theta \\ M_{Bm} = M_{sr} \cos \theta \end{cases}. \tag{7}$$

Therein, M_{sr} is the coefficient of mutual inductance between the rotors.

By plugging (7) into (6), we can obtain:

$$T_e = N_r \left[L_1 \sin 2\theta \left(i_A^2 - i_B^2 \right) - 2 i_A i_B L_1 \cos 2\theta \right] + N_r I_m M_{sr} \left(i_A \cos \theta - i_B \sin \theta \right). \tag{8}$$

This is the characteristics of torque in the case when the two-phase hybrid stepper motor doesn't consider the effect from the magnetic leakage and the saturation of a magnetic circuit in the motor circuit. According to the characteristics of torque, the different control schemes of a stepper motor can be obtained as: one is the subdivided control, another one is the vector control. This system model can realize the stepper motor control accuracy and fast responsiveness through carrying the subdivided driving technology, as well as the suitable acceleration and deceleration curve algorithm.

The simulation model of the two-phase hybrid stepper motor open-loop control system is set up in Fig. 1 by Matlab/Simulink.

In Fig. 1, the simulation model is mainly composed of 4 parts: the hybrid stepper motor module, which is the simplified model of a two-phase hybrid stepper motor, it is set up by Formula (1) and Formula (2); the PWM module, which is the input current signal converted to a PWM wave; converter A, the B module which represent two PWM inverters; the ACC/DEC curve – subdivision circuit module, which is the designed acceleration and deceleration curves, as well as a microstep subdivided driving module. This module will be discussed specifically in the following content.

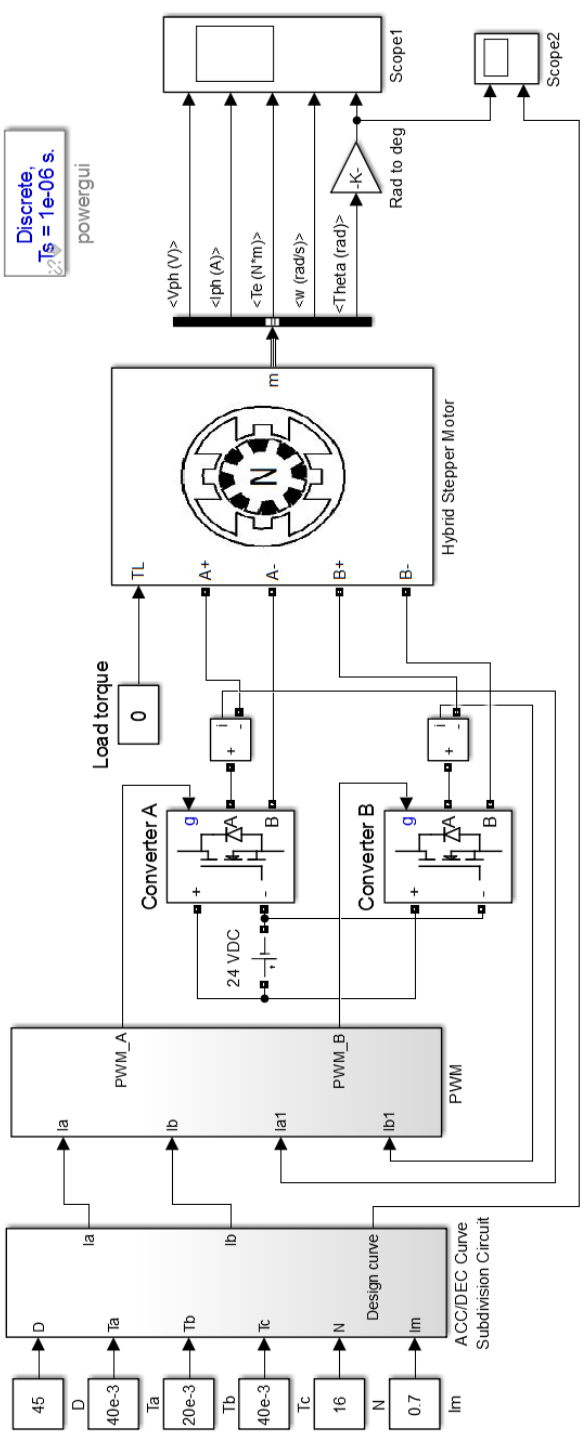

Fig. 1. Model of stepper motor open-loop control system

3. Subdivision driving technology

Subdivision driving technology subdivides the stepper angle of a stepping motor, so as to let the stepper motor control system have the higher resolution. A two-phase hybrid stepper motor needs to make the composite vector of each phase winding current to do the uniform amplitude of constant rotational motion in the space through the quasi sinusoidal current in the two-phase winding.

The common formula [13] of the phase current in the subdivision control is:

$$\begin{cases} I_a = I_r \times \cos\alpha \\ I_b = I_r \times \sin\alpha \end{cases}. \tag{9}$$

Therein, I_r is the rated current of the motor, α is the current real-time angle, its computing method is:

$$\alpha = \frac{\pi}{2N} \times S. \tag{10}$$

Therein, N is the number of subdivision, S is the worked steps of the stepper motor.

Respectively carry out the simulation for 4 subdivisions, 8 subdivisions and 16 subdivisions based on the established stepper motor control system model, analyze the relationships among the stepper angle and the number of subdivision in each subdivision work way, as shown in Fig. 2.

From the simulation waveform figure, we can see that the two-phase current shows the obvious quasi sinusoidal waveform, the stepper angle decreases with the increasing number of

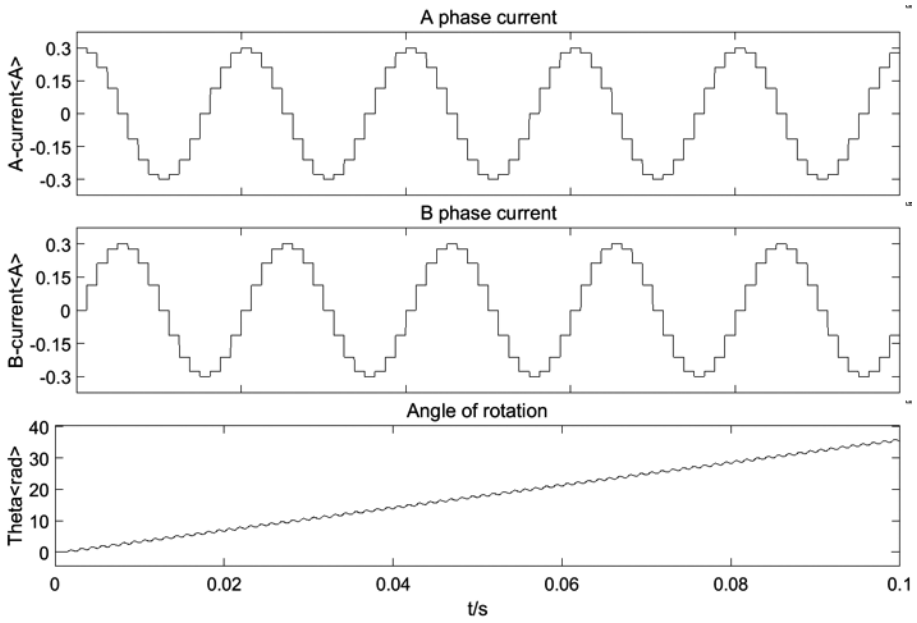

(a) Phase diagram of two phase current and rotation angle under 4 subdivision mode

Fig. 2.

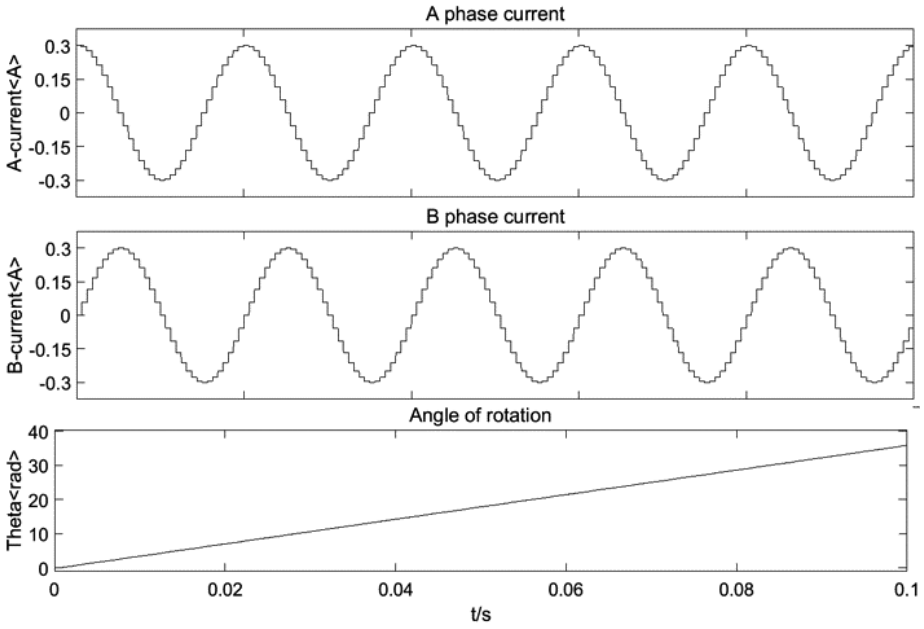

(b) Phase diagram of two phase current and rotation angle under 8 subdivision mode

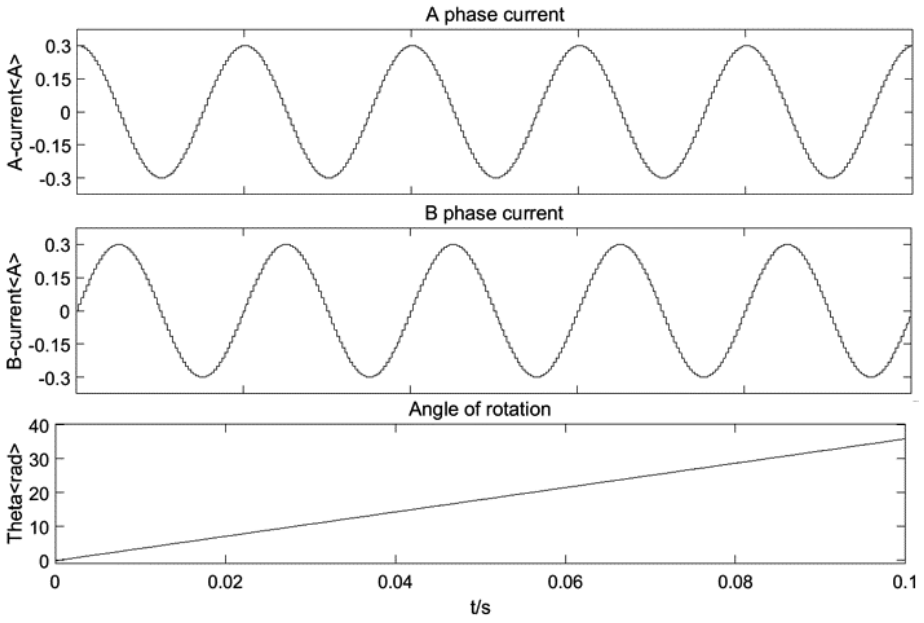

(c) Phase diagram of two phase current and rotation angle under 16 subdivision mode

Fig. 2. Three subdivision modes of current and rotation angle

subdivisions, the system resolution becomes higher, and the actual rotation angle of the motor can reach the targeted angle in each subdivision work way.

4. Acceleration and deceleration curve design

4.1. Trapezoidal acceleration and deceleration curves

The trapezoidal acceleration and deceleration curves are designed as in Fig. 3, the whole process is divided into acceleration, uniform velocity and deceleration. The stepper motor starts, runs n_A steps by the acceleration β, and then accelerates the speed to the maximum speed w_m, it reduces the speed by the same acceleration after running n_B steps by the constant speed, the stepper motor stops to work after n_C steps. We know the total steps n, total control period T, as well as n_A, n_B, n_C and other parameters, we need to calculate the acceleration β, and the stepper period T_i of every step in each running stage.

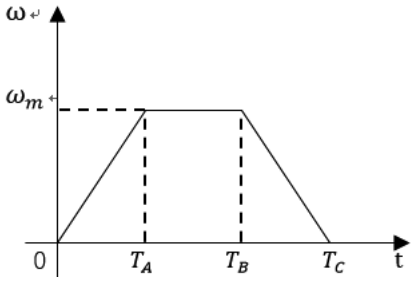

Fig. 3. Trapezoidal acceleration and deceleration curve

In the acceleration stage, the relationships between the angular velocity and angular displacement are as follows:

$$\omega t + \frac{1}{2}\beta t^2 = \theta. \tag{11}$$

Initial velocity $\omega = 0$, after the discretization, can get:

$$\frac{1}{2}\beta t_i^2 = \theta_i = i\delta. \tag{12}$$

Therein, θ_i is the rotated angle of the motor after sending the i pulse; δ is the stepper angle.

From Formula (12), the time t_i to finish sending the i pulse in the acceleration stage, and the time t_{i-1} to finish sending the $(i-1)$ pulse are as follows:

$$\begin{cases} t_i = \sqrt{\dfrac{2\delta i}{\beta}} \\ t_{i-1} = \sqrt{\dfrac{2\delta(i-1)}{\beta}} \end{cases}. \tag{13}$$

From the angular velocity-time curve diagram, we see that:

$$\frac{1}{2}\omega_m T_A = \varphi_A\,. \tag{14}$$

Therein, T_A, φ_A are, respectively, the required time and rotated angle in the acceleration stage. From Formula (14), we can get:

$$\beta = \frac{\omega_m}{T_A} = \frac{2\varphi_A}{T_A^2}. \tag{15}$$

To sum up, the period T_i of the i pulse can be obtained from Formula (13) and Formula (15):

$$T_i = t_i - t_{i-1} = T_A\sqrt{\frac{1}{n_A}}\left(\sqrt{i} - \sqrt{i-1}\right). \tag{16}$$

Therein, the value range of i is $1, 2, 3, \ldots, n_A$.

The derivation of every stepper period in the uniform velocity and deceleration stage are similar to the acceleration stage, the stepper period of the i pulse in the uniform velocity and deceleration stage are, respectively:

$$T_j = \frac{T_B}{n_B} \quad j \in \{1, 2, \ldots, n_B\}, \tag{17}$$

$$T_k = T_C\left[\sqrt{\frac{n_C - i + 1}{n_C}} - \sqrt{\frac{n_C - i}{n_C}}\right], \quad k \in \{1, 2, \ldots, n_C\}, \quad (n_A + n_B + n_C = n). \tag{18}$$

4.2. Parabolic acceleration and deceleration curves

Parabolic acceleration and deceleration curves are designed as in Fig. 4; the whole process is divided into acceleration, uniform velocity and deceleration.

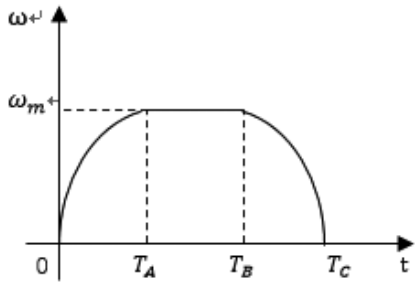

Fig. 4. Parabolic acceleration and deceleration curve

Due to the derivation method of every stepper period T_i, in each stage it is similar to the parabolic acceleration and deceleration curves, every stepper period of all the parabolic stages is, respectively:

$$T_i = T_A n_A^{-\frac{2}{3}}\left[i^{\frac{2}{3}} - (i-1)^{\frac{2}{3}}\right], \quad i \in \{1, 2, \ldots, n_A\}, \tag{19}$$

$$T_j = \frac{T_B}{n_B}, \quad j \in \{1, 2, \ldots, n_B\}, \tag{20}$$

$$T_k = T_C n_C^{-\frac{2}{3}}\left[(n_C - k + 1)^{\frac{2}{3}} - (n_C - k)^{\frac{2}{3}}\right], \quad k \in \{1, 2, \ldots, n_C\}, \quad (n_A + n_B + n_C = n). \tag{21}$$

From the above computing process, the stepper pulse sequence can be easily obtained when the stepper motor runs different acceleration and deceleration curves, speed, position curve and others.

5. Simulation analysis

In this paper we aim at researching the angular displacement output from the stepper motor, we carry out the simulation for the above two types of acceleration and deceleration curves by the established stepper motor open-loop control system model. The stepper motor parameters: the number of rotor teeth is 50, the stepper angle is 1.8°, the maximum output torque is $6.5 \cdot 10^{-3}$ N·m, the working voltage is 24 V, the moment of inertia of the motor shaft is $0.58 \cdot 10^{-7}$ kg·m^2, the viscous damper is $1 \cdot 10^{-4}$ kg·m/s. The rotation time from the motor start to stop is 100 ms, including the acceleration; uniform velocity and deceleration time are, respectively, 40 ms, 20 ms and 40 ms.

When the targeted angular displacement of the stepper motor is designed as 45°, the simulation results of the acceleration and deceleration curves in two ways are as shown in Fig. 5.

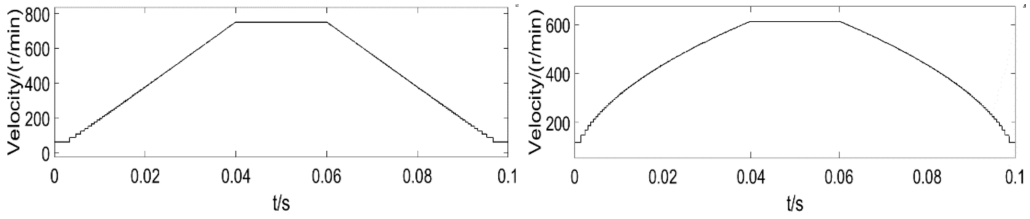

(a) Trapezoidal acceleration and deceleration curve (b) Parabolic acceleration and deceleration curve

Fig. 5. Two acceleration and deceleration curves

Respectively adopt these two types of speed curves as the input of the simulation system to get all kinds of running curves of the stepper motor. The simulation result shows that the control system is adopted by the trapezoidal acceleration and deceleration curves, the maximum in-step angle of stepper motor is 820° within a 100 ms control period; and the maximum in-step angle is 990° when adopting the parabolic acceleration and deceleration curves. When the stepping motor is in the maximum in-step angle process, the simulation result of the relationships between the motor output angular displacement and time of these two kinds of velocity curves looks as it is shown in Fig. 6, including the full line that represents the targeted angular displacement curve; the dotted line represents the actual angular displacement curve. Carry out the differential

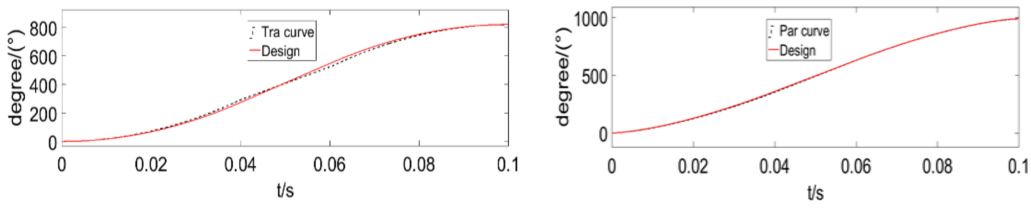

(a) Trapezoidal acceleration and deceleration curve (b) Parabolic acceleration and deceleration curve

Fig. 6. Relationship of the stepping motor's output angle displacement and the time

treatment for the actual angular displacement and targeted angular displacement, therefore, the position tracking error simulation diagram in the stepper motor running process is obtained as shown in Fig. 7.

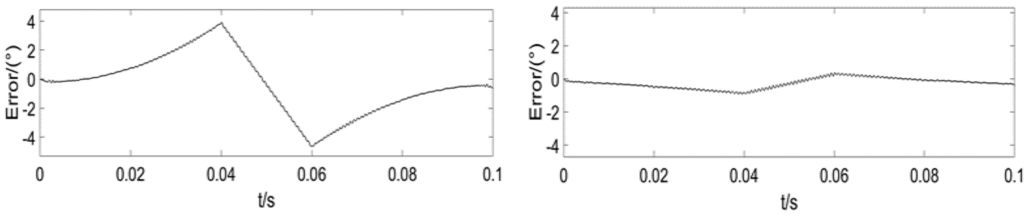

(a) Trapezoidal acceleration and deceleration curve (b) Parabolic acceleration and deceleration curve

Fig. 7. Simulink results of position tracking error

The simulation result shows that the parabolic acceleration and deceleration curves have a larger in-step rotation angle than the trapezoidal acceleration and deceleration curves within the same control period, and at the same time the position tracking error is smaller in the intermediate process.

6. Experimental verification

The two types of velocity curves described above have undergone experimental verification with the use of the STM32 demoboard. The driving stepper motor parameters are basically fit with the stepper motor in the simulation model, the number of rotor teeth is 50, the stepper angle is 1.8°, the maximum output torque is $6.5 \cdot 10^{-3}$ N·m, the working voltage is 24 V, the moment of inertia of the motor shaft is $0.58 \cdot 10^{-7}$ kg·m^2, the number of the microstep subdivision of the driving circuit is 16, the rotation time from the motor start to stop is 100 ms, including the acceleration, uniform velocity and deceleration time are, respectively, 40 ms, 20 ms and 40 ms.

The maximum in-step angular displacement of two kinds of velocity curves and their corresponding error curves are shown in Fig. 8 and Fig. 9. From the diagrams we can see that when the

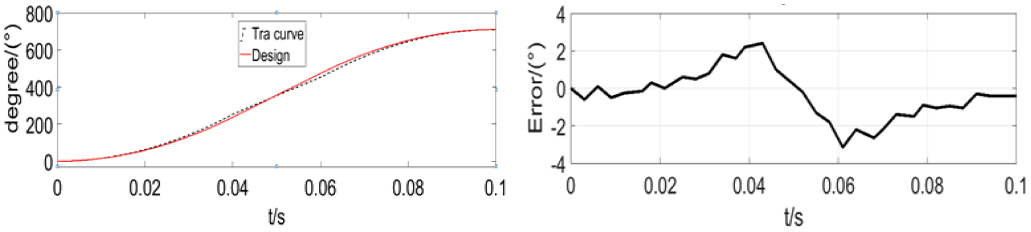

(a) Angular displacement curve of 710 degree of stepping motor (b) Position error curve of 710 degree of stepping motor

Fig. 8. Angle displacement and error curves of 710 degree based on trapezoidal profile

control system is adopted by the trapezoidal acceleration and deceleration curves, the maximum in-step angle of the stepper motor is 710° within 100 ms control period; and the maximum in-step angle is 900°. When adopting the parabolic acceleration and deceleration curves, it enhances around 27% than the trapezoidal acceleration and deceleration curves, and at the same time the position tracking error is smaller in the intermediate process.

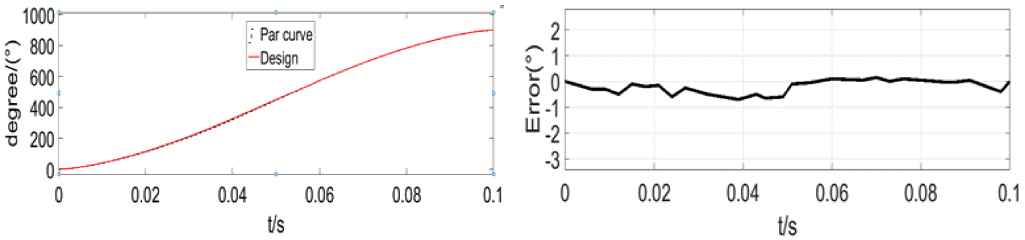

(a) Angular displacement curve of 900 degree of stepping motor

(b) Position error curve of 900 degree of stepping motor

Fig. 9. Angle displacement and error curves of 900 degree based on parabolic profile

The experimental test is also carried out with the other rotation angles, the maximum value of the angular displacement error in the intermediate process, in the case of these two kinds of velocity curves, is at different rotation angles and it is summarized in Table 1. The parabolic acceleration and deceleration curves have a larger in-step rotation angle than the trapezoidal curves within the same control period, and at the same time the angular displacement error in the intermediate process decreases. The experiment is basically fit with the simulation result and the rules, the accuracy of the foregoing theoretical analysis has been proved. The application of parabolic acceleration and deceleration way causes that the stepper motor open-loop control performance shows an obvious improvement.

Table 1. Angle displacement errors at different degrees

Angle	**540°**	**630°**	**710°**	**800°**	**900°**
Trapezoidal	−2.4~2.0	−2.9~2.3	−3.2~2.4	–	–
Parabolic	−0.5~0.15	−0.5~0.2	−0.7~0.2	−0.7~0.2	−0.8~0.2

7. Conclusion

1) According to the mathematical model of a two-phase hybrid stepper motor, microstep subdivision driving technology and the acceleration and deceleration curve technology, the simulation model of the two-phase hybrid stepper motor is set up, and the working principle of microstep subdivided driving technology can be used for the real-time online computing acceleration and deceleration curve algorithm after carrying out the discussion.

2) The simulation respectively analyzes the two-phase current and rotation angle of the stepper motor in three kinds of working ways, the simulation shows that the working steps of the stepper motor within the unit time increase, the unit stepper angle becomes smaller with the increasing number of subdivision, the stepper motor system can obtain the higher resolution, smaller pulse equivalent, in addition, it can obviously decrease or eliminate the low frequency vibration and noise of the stepper motor.

3) The simulation analyzes the control performance of trapezoidal acceleration and deceleration curves and parabolic acceleration and deceleration curves. The simulation shows that the maximum in-step angle of parabolic acceleration and deceleration curves reaches to 990° within 100 ms control period, it enhances 21% than the trapezoidal acceleration and deceleration curves; and at the same time its position tracking error is smaller. It shows that the parabolic acceleration and deceleration curves have faster dynamic response speed and better open-loop control characteristics.

4) The experiment verifies the control performance of trapezoidal, parabolic speed curves. The experimental result shows that the maximum in-step angle of the parabolic speed curve is 900° within the same control period, it enhances around 27% than the trapezoidal speed curve, and at the same time its angular displacement error decreases relatively. The simulation and experiment show that the parabolic acceleration and deceleration curves have the faster dynamic response ability.

Acknowledgement

This work is supported by the Wuhan science and technology support program (No. 2017010201010137) and the National Key Research and Development Program of China (No. 2016YFC0401702).

References

[1] Yole Development, *MEMS Front-End Manufacturing Trends*, Research and Markets, vol. 03, pp. 96–114 (2013).

[2] Wang L., Xin X., Zhu L., *A widely tunable fiber ring laser with closed loop control based on high-precision stepper motor*, Optoelectronics Letters, vol. 03, pp. 169–172 (2016).

[3] Wang Q., Lu Q., *High performance closed loop drive of two phase hybrid stepping motor*, Zhejiang Province, Zhejiang Sci-Tech University (2017).

[4] Stănică D.-M., Lita I., Oproescu M., *Comparative analysis of stepper motors in open loop and closed loop used in nuclear engineering*, IEEE 23rd International Symposium for Design and Technology in Electronic Packaging (2017).

[5] Na Deng, Hong Yingcao, Cun Ganghu, *Application of stepper motor subdivision drive in transformation of CA6140 lathe*, IEEE 11th Conference on Industrial Electronics and Applications (2016).

[6] Wonhee Kim, Donghoon Shin, Youngwoo Lee, Chung Choo Chung, *Simplified torque modulated microstepping for position control of permanent magnet stepper motors*, Mechatronics, vol. 35, no. 5, pp. 162–172 (2016).

[7] Lyshevski S.E., *Microstepping and high-performance control of permanent-magnet stepper motors*, Energy Conversion and Management, vol. 85, no. 9, pp. 245–253 (2014).

[8] Wonhee Kim, Donghoon Shin, Chung Choo Chung, *The Lyapunov-based controller with a passive nonlinear observer to improve position tracking performance of microstepping in permanent magnet stepper motors*, Automatica, vol. 48, no. 12, pp. 3064–3074 (2012).

[9] Wonhee Kim, Donghoon Shin, Chung Choo Chung, *Microstepping with Nonlinear Torque Modulation for Permanent Magnet Stepper Motors*, IEEE Transactions on Control Systems Technology, vol. 21, no. 5, pp. 1971–1979 (2013).

[10] Bo Wang, Wei Tang, Ji Xiandong, Fengh Wang, *Positioning-control Based on Trapezoidal Velocity Curve for High-precision Basis Weight Control Valve*, Paper and Biomaterials, vol. 2, pp. 42–50 (2017).

[11] Hasanien H.M., *FPGA implementation of adaptive ANN controller for speed regulation of permanent magnet stepper motor drives*, Energy Conversion and Management, vol. 52, no. 2, pp. 1252–1257 (2011).

[12] Ji Shuai, Hu Tianliang, Zhang Chengrui, Sun Shuren, *A parametric hardware fine acceleration/deceleration algorithm and its implementation*, The International Journal of Advanced Manufacturing Technology, vol. 63, no. 9, pp. 1109–1115 (2012).

[13] Xianmin Wei, *Acceleration and Deceleration Control Design of Step Motor Based on TMS320F240*, Procedia Engineering, vol. 15, no. 1, pp. 501–504 (2011).

[14] Muñiz C., Levi R., Rodríguez M.B.F.B., Varona P., *Real-time control of stepper motors for mechanosensory stimulation*, Journal of Neuroscience Methods, vol. 172, no. 1, pp. 105–111 (2008).

[15] Liang Zhai, *Research on new control strategy of two phase hybrid stepping motor*, Zhejiang Province, Zhejiang University (2011).